ANALYSIS OF THE INFLUENCE OF GEOMETRIC AND VENTILATION FACTORS ON INDOOR POLLUTANT DISPERSION: A NUMERICAL STUDY

Agnese Pini[1], Tommaso Vigilante[1], Livia Grandoni[1], Giovanni Leuzzi[1], Armando Pelliccioni[2] and Paolo Monti[1]

[1]DICEA, University of Rome "La Sapienza", Rome, Italy
[2]INAIL-DIMEILA, Monteporzio Catone, Rome, Italy

Abstract: The aim of this study is to delineate the role played by natural ventilation and room geometry on indoor dispersion. To this end, particle material (PM) concentration fields obtained using Computational Fluid Dynamics (CFD) concerning a series of ideal cases regarding parallelepiped rooms of different sizes and inlet velocities at the openings have been analysed. The numerical results have been compared with the concentrations obtained using a Box Model based on the mass balance. The results show a reasonably good agreement between the emptying times of the rooms calculated by the CFD and the Box Model, particularly when the room is square shaped. It was also found that the emptying time assumes an almost constant value once normalized with the inlet velocity and room diagonal. Since these are known values, it is possible to infer the emptying time avoiding the use of highly time-consuming numerical simulations.

***Key words**: Box model; CFD; DPM; Indoor; Particle dispersion modelling.*

INTRODUCTION

Air quality is one of the fundamental aspects for the well-being and comfort of people both indoors and outdoors. For this reason, studies aiming at improving air quality has become one of the main topics covered by the scientific community (Kalimeri et al. 2019; Pelliccioni et al. 2020). The event that has affected our society in the last two years (e.g., Campanelli et al. 2021, Iannarelli et al. 2022) has increased the hours spent by the population in confined environments. In fact, people spend on average approximately 90% of their time indoors, where the concentrations of some pollutants are often 2−5 times higher than typical outdoor concentrations (U.S. EPA 2021). For this reason, studies of indoor pollutant dispersion have become crucial to ensure a healthy life for people. The objective of this paper is to investigate particle material (PM) dispersion indoors using Computational Fluid Dynamics (CFD), which has proved to be useful in the analysis of indoor PM dispersion and indoor-outdoor interaction (e.g., Blocken 2015).

The simulations were carried out by examining ideal cases consisting of parallelepiped rooms of different sizes and injection characteristics of PM from an opening. The PM concentration is obtained via the mixed Eulerian-Lagrangian method, i.e., the dispersed phase is calculated by determining the trajectories of the particles dispersed in the continuous phase (Lagrangian description). Particular attention is payed to the filling and emptying phases of the room and the way in which they depend on the room size and boundary conditions. With regard to the emptying phase, the CFD results will be compared to those obtained by means of a simple Box Model based on the mass balance.

CFD SIMULATIONS: COMPUTATIONAL DOMAINS AND SETTINGS

Four different parallelepiped rooms were considered in the analysis (Figure 1). For each geometry the rooms were set up with a different number of windows but only one of these, always in the same position, was considered as open. In particular, the rooms have two openings placed on the two opposite walls: a window of size 1.4x1.4 m^2, which represents the inlet, positioned one meter from the right sidewall; a door of area 1x2 m^2, which represents the outlet, located one meter from the left sidewall. The CFD model ANSYS Fluent 18.2 (ANSYS, 2011), was employed to simulate the airflow and evaluate PM dispersion

for the four geometrical configurations and different boundary conditions. GAMBIT 2.4.6 was used to build the (structured) meshes (cell width 7.5 cm). The main characteristics of the four geometries, hereinafter C1, C2, C3 and C4, are listed in Table 1. Grid independence analysis (not shown) allows us to affirm that all the four grids provide nearly grid-independent results.
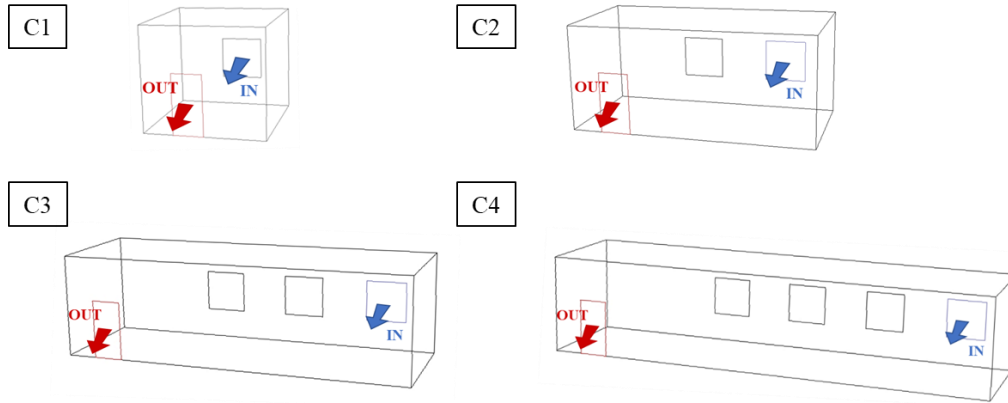
Figure 1. Schematics of the four rooms considered in the analysis.

|	Area [m^2]	Height [m]	Volume [m^3]	Cell number [-]	Cell size [m]	Node number [-]
C1	16	3.5	56	132023	0.075	139968
C2	32	3.5	112	266537	0.075	279936
C3	48	3.5	168	398560	0.075	417312
C4	64	3.5	224	554688	0.075	554688

Table 1. Main characteristics of the four geometries

The RANS equations, along with the re-normalization group (RNG) k-ε model (e.g., Xu and Wang 2017) were employed to predict the average velocity field inside the room. Here, k is turbulence kinetic energy and ε its dissipation rate. The Discrete Phase Model (DPM) implemented in Fluent was used to simulate injection and diffusion of the PM. The DPM simulates the continuous and the discrete phases by means of the Eulerian and the Lagrangian approach, respectively. The interaction between the two phases is taken into account by the DPM coupling the solution along with an unsteady particle tracking (time step 1 s). The residual values used to control the solution convergence have been set equal to 10^{-6} for continuity, the three velocity components, k and ε.

For each geometry, the simulations were carried out in steady conditions for four values of the inlet velocity (i.e., U_{IN}=0.3, 0.5, 0.7 and 0.9 m s^{-1}) normal to the window for a total of 16 runs. A PM 1 μm in diameter and 1650 kg m^{-3} in density has been considered for the analysis. The particle velocity at the inlet has been assumed evenly distributed and equal to that of air. A constant PM flow rate of 10^{-8} kg s^{-1} has been considered. For all the 16 runs, after the stationary condition for the velocity field has been obtained, the PM is injected from the window (filling phase). Once a steady condition for the PM concentration has been reached, clean air is again blown through the window (emptying phase).

RESULTS AND DISCUSSION
By way of example, Figure 2 shows the velocity magnitude simulated at z=1.75 m above the floor for the four geometries with U_{IN}=0.3 m s^{-1}. It can be noted that, except in case C1, an area with very low velocity occurs at the right of the entering flow. The size of the low-velocity area increases passing from the smallest to the largest room. In fact, while for C1 the air after entering the window continues to flow nearly straight towards the door, in the other cases the air reaches the opposite wall and then flows parallel to it before exiting the door, giving rise to a low-velocity area near the wall opposite the door. Similar considerations can be drawn from the analysis of the velocity fields obtained using the other three U_{IN}.
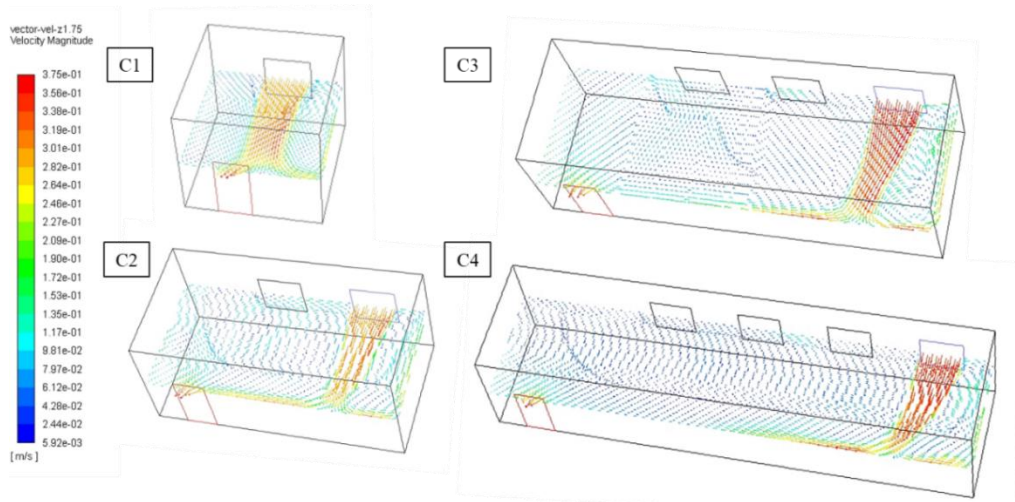
Figure 2. Velocity magnitude simulated at 1.75 m above the floor level for the four geometries (U_{IN}=0.3 ms^{-1}).

Figure 3a shows the time histories of PM concentration − spatially averaged in the room − simulated for case C1 for the four U_{IN}. The PM injection at the window starts after the flow field has reached the steady condition (t=0) and lasts 1800 s (filling phase), an interval long enough for the concentration field to reach the steady state condition in all the investigated cases. Then, clean air enters again from the window (emptying phase) for 1800 s.
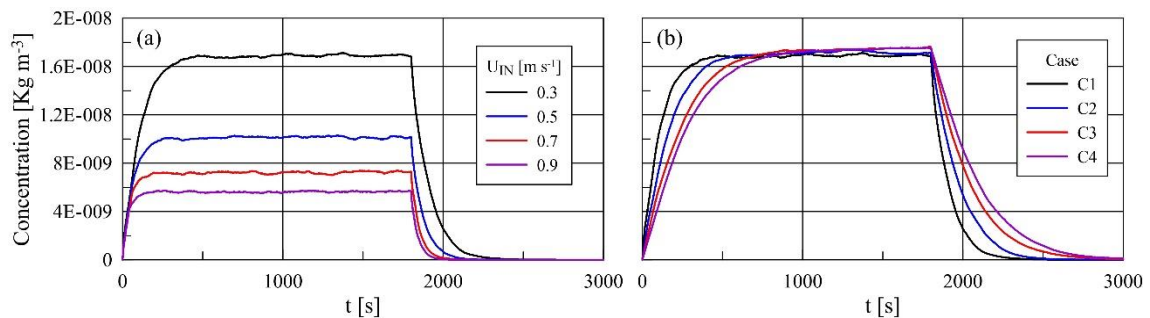
Figure 3. (a) Time histories of the average PM concentration for case C1 as a function of the inlet velocity U_{IN}.
(b) Time histories of the average concentration for U_{IN}=0.3 ms^{-1} for the four study cases.

As expected, the average concentration decreases as velocity increases and so does the time (T_F) needed to reach the steady condition for the concentration during the filling phase. The same applies during the emptying phase, i.e., the higher the inlet velocity the shorter the emptying time (T_E).

Figure 3b depicts the time histories of the average PM concentrations calculated for the four geometries when U_{IN}=0.3 m s^{-1}. It is apparent that the larger the room the longer T_E and T_F. Figure 4 depicts filling and emptying times calculated for the 16 runs. It is possible to summarize what was observed above: U_{IN} being equal, T_E and T_F increase as the size of the room increases; on the other hand, area of the room being equal, T_E and T_F decrease as U_{IN} increases.

Let us now consider the Box Model. Most of them assume that the pollutant concentration is homogeneous within the control volume considered for the analysis and that the pollutant mixes instantaneously. Hence, it is possible to calculate the pollutant concentration based on the mass balance, considering both natural ventilation and infiltration phenomena.
With the view to simplify the model, particle sedimentation can be neglected, as the particle size is small; furthermore, source terms and resuspension can be also assumed negligible. Under these hypotheses, the

mass balance can be written as (e.g., Pini et al. 2020):

$$\frac{dC_{IN}}{dt} = a(PC_W - C_{IN})$$ (1)
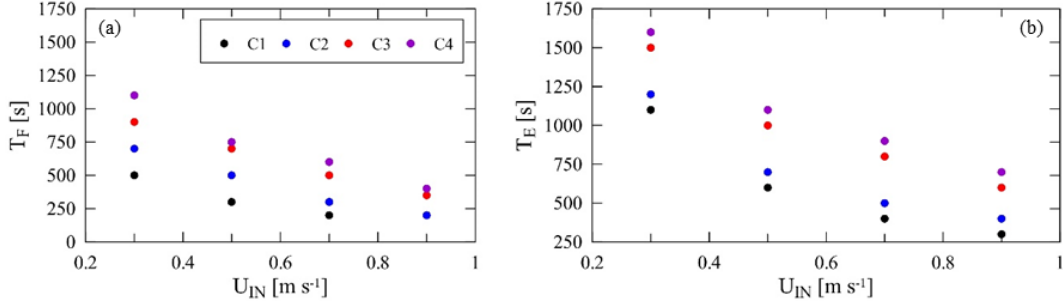
Figure 4. Filling time (a) and emptying time (b) as a function of the inlet velocity and room geometry.

Here, a is the air exchange rate, defined as the number of air changes in the room per unit of time (determined as the ratio between the inlet flow rate, $Q_{IN}=U_{IN}\cdot$(window area), and the room volume, V), P is the infiltration factor (P=1 for open window), C_W and C_{IN} are the inlet and the indoor concentration, respectively. In discrete form:

$$C_{IN}^{(i+1)} = C_{IN}^{(i)} + a^{(i)}\big(C_W^{(i)} - C_{IN}^{(i)}\big)\Delta t$$ (2)

where i is the iteration step and Δt the time interval. The quantity $\Delta = (T_E|_{BM} - T_E|_{CFD})/T_E|_{BM} \cdot 100\ [\%]$ calculated for the 16 simulations is depicted in Figure 5. Here $T_E|_{BM}$ and $T_E|_{CFD}$ are the emptying time calculated with the Box Model and the CFD, respectively. In order to avoid uncertainties in T_E determination, in what follows T_E is assumed as the time needed to reach 10% of the room concentration at the steady state. Assuming that Fluent provides more correct results than the Box Model (we may only speculate that since no experimental data to validate the models are available), the Box Model works reasonably good for regular geometries, in which the hypothesis of uniform concentration is more reasonable. In fact, for C1 and C2 the differences between the emptying times calculated by the Box Model and the CFD are negligible irrespective of the inlet velocity ($\Delta<2\%$). In contrast, when the geometries are far to be cubic, i.e., C3 and C4, the departures from the results obtained with the CFD are greater, probably due to the fact that the hypothesis of uniform concentration is not appropriate. However, the differences between the two models remain well below 10%, which is an acceptable threshold given the simplifying hypothesis adopted in equation 1.
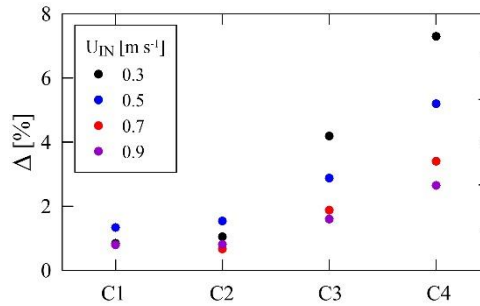
Figure 5. Percentage difference $\Delta = (T_E|_{BM} - T_E|_{CFD})/T_E|_{BM} \cdot 100$ for the 16 simulations.

Finally, an attempt was made to normalize the emptying time. Three different time scales, T_s, were taken into consideration, i.e., V/Q_{IN}, D/U_{IN} and k/ε, (where V and D are, respectively, volume and diagonal of the room), from which it is possible to determine the ratio $\alpha = T_E/T_s$. It is important to observe that $T_s = V/Q_{IN}$ and $T_s = D/Q_{IN}$ can be calculated *a priori* as they depend on room geometry and boundary conditions (known quantities). Conversely, $T_s = k/\varepsilon$ can only be calculated starting from CFD simulations,

thus being less applicable than the first two. The values of α were analyzed considering all the three time scales for all the considered geometries. Among the three time scales, $T_S = D/Q_{IN}$ seems to be the best choice (i.e., lower variations of α) for all the 16 simulations. The values of α obtained for the 16 simulations are listed in Table 2. By averaging over all the 16 simulations, a value of α close to 12.4 is obtained.

	U_{IN}=0.3 m s^{-1}	U_{IN}=0.5 m s^{-1}	U_{IN}=0.7 m s^{-1}	U_{IN}=0.9 m s^{-1}	$\bar{\alpha}$
C1	12.9	13.1	14.4	15.1	**13.9**
C2	12.4	11.9	13.1	12.2	**12.4**
C3	12.1	11.9	12.3	12.1	**12.1**
C4	11.1	10.7	11.3	11.4	**11.1**

Table 2. Values of $\alpha = T_E/T_S = T_E U_{IN}/D$ for the 16 simulations. The last column reports α averaged over the four room geometries.

In conclusion, two interesting features were found in this work: (a) for the type of room geometry considered in the analysis, the PM concentration simulated analytically by a simple Box Model are comparable to those simulated by a CFD model; (b) when the window-door distance is similar to the room diagonal, it is possible to determine the emptying time without the need to conduct computationally expensive numerical simulations.

Further work is in progress investigating other geometries and inlet conditions in order to generalize the results.

REFERENCES
ANSYS. (2011). ANSYS FLUENT User's Guide – Release 14.0. ANSYS. Canonsburg, PA.
Blocken, B., 2015: Computational Fluid Dynamics for urban physics: Importance, scales, possibilities, limitations and ten tips and tricks towards accurate and reliable simulations. *Build. Environ.,* **91**, 219-245.
Chen, C. and B. Zhao, 2011: Review of relationship between indoor and outdoor particles: I/O ratio, infiltration factor and penetration factor. *Atmos. Environ.*, **45**, 275-288.
Chen, C., B. Zhao, W. Zhou, X. Jiang, and Z. Tan, 2012: A methodology for predicting particle penetration factor through cracks of windows and doors for actual engineering application. *Build. Environ.,* **47**, 339-348.
Campanelli, M, A. M. Iannarelli, G. Mevi, S. Casadio, H. Diémoz, S. Finardi, A. Dinoi, E. Castelli, A. di Sarra, A. Di Bernardino, G. Casasanta, C. Bassani, A. M. Siani, M. Cacciani, F. Barnaba, L. Di Liberto, S. Argentini, 2021: A wide-ranging investigation of the COVID-19 lockdown effects on the atmospheric composition in various Italian urban sites (AER – LOCUS). *Urban Clim.*, **39**, 100954.
Iannarelli, A.M., A. Di Bernardino, S. Casadio, C. Bassani, M. Cacciani, M. Campanelli, G. Casasanta, E. Cadau, H. Diemoz, G. Mevi, A.M. Siani, M. Cardaci, 2022: The Boundary Layer Air Quality-Analysis Using Network of Instruments (BAQUNIN) Supersite for Atmospheric Research and Satellite Validation over Rome Area. *Bull. Am. Meteorol. Soc.*, **103**, E599-E618.
Kalimeri, K., J. G. Bartzis, I. A. Sakellaris, E. de Oliveira Fernandes, 2019: Investigation of the PM2.5, NO2 and O3 I/O ratios for office and school microenvironments. *Environ. Res.*, **179**, 108791.
Pelliccioni A., et al., 2020: Integrated evaluation of indoor particulate exposure: The Viepi project. *Sustainability*, **12**, 9758.
Pini, A., L. Grandoni, G. Leuzzi, P. Monti, A. Di Bernardino, A. Pelliccioni, M. Gherardi, G. Cattani, A. Di Menno di Bucchianico, 2020: A Simplified Analytical Model of Ultrafine Particle Concentration within an Indoor Environment. *IOP Conference Series: Earth and Environmental Science* 489 (1).
Xu, G. and J. Wang, 2017: CFD modeling of particle dispersion and deposition coupled with particle dynamical models in a ventilated room. *Atmos. Environ.*, **166**, 300-314.
U.S. Environmental Protection Agency, 2021: Indoor air quality: What are the trends in indoor air quality and their effects on human health? https://www.epa.gov/report-environment/indoor-air-quality (accessed 4th July 2022).